4224 *Inorg. Chem.* **2010**, *49*, 4224–4231
DOI: 10.1021/ic9025574

Inorganic Chemistry
Article

Hydration Properties of the Bromide Aqua Ion: the Interplay of First Principle and Classical Molecular Dynamics, and X-ray Absorption Spectroscopy

Paola D'Angelo,*,† Valentina Migliorati,† and Leonardo Guidoni‡

†*Dipartimento di Chimica, Università di Roma "La Sapienza", P.le A. Moro 5, 00185 Roma, Italy, and*
‡*Dipartimento di Chimica, Ingegneria Chimica e Materiali, Università degli Studi dell'Aquila, via Campo di Pile, zona industriale di Pile, 67100, L'Aquila, Italy*

Received December 22, 2009

The hydration properties of the bromide aqua ion have been investigated using state of the art density functional theory (DFT) based molecular dynamics with dispersion-corrected atom-centered pseudopotentials for water and classical molecular dynamics simulations. The reliability of the theoretical results has been assessed by comparing the attained structural results with the extended X-ray absorption fine structure (EXAFS) experimental data. The EXAFS technique is mainly sensitive to short distances around the bromine atom, and it is a direct probe of the local solvation structure. The comparison shows that the DFT simulation delivers a good description of the EXAFS experimental signal, while classical simulation performs poorly. The main reason behind this is the neglect of polarization effects in the classical ion−water interaction potentials. By taking advantage of the reliable information on the Br^- local hydration structure it has been possible to highlight the contribution of hydrogen atoms to the EXAFS spectra of halide aqueous systems.

1. Introduction

The solvation properties of ions and the role of the surrounding water molecules are important throughout biology and chemistry.[1,2] While much experimental and theoretical work has been devoted to characterize the structural and dynamical behavior of cations in water[3−7] the hydration properties of halides are still the subject of intense debate.[8−15] For the bromide ion the hydration number as determined by X-ray and neutron diffraction and X-ray absorption is in the range 6−7.4[8−15] and, as found for other halide ions, it is very difficult to establish the number of water molecules belonging to the first coordination shell because of its diffuse character.[8−15] The Br−O first shell average bond length determined by X-ray diffraction is in the range 3.19−3.40 Å.[8−15] These scattered results underline the difficulty of defining the halide coordination shells also as a consequence of the fast water exchange between the first and second hydration shells. The experimental residence time is generally estimated to be very short (less than 5 ps).[16] A K-edge extended X-ray absorption fine structure (EXAFS) study of bromide ions in aqueous solutions has been carried out using classical Molecular Dynamics (MD)simulations.[9] The obtained Br−O radial distribution function was used with the integral formulation of the EXAFS equation to simulate the EXAFS theoretical signal which was found to be in very good agreement with the experimental data. While this approach did not allow to get the detailed orientation of water molecules around the bromide ion (the H atoms were neglected), it did provide an oxygen coordination number (6.9) and first shell distance (3.34 Å), well within the range of previous studies.[8] The same approach was used by Wallen et al.[12] who extended the range of temperatures into the supercritical

*To whom correspondence should be addressed. E-mail: p.dangelo@caspur.it.

(1) Ando, K.; Hynes, J. T. *J. Phys. Chem. B* **1997**, *101*, 10464–10478.
(2) Laage, D.; Hynes, J. T. *Proc. Proc. Natl. Acad. Sci.* **2007**, *104*, 11167–11172.
(3) Chillemi, G.; D'Angelo, P.; Pavel, N. V.; Sanna, N.; Barone, V. *J. Am. Chem. Soc.* **2002**, *124*, 1968–1976.
(4) D'Angelo, P.; Migliorati, V.; Mancini, G.; Barone, V.; Chillemi, G. *J. Chem. Phys.* **2008**, *128*, 84502–84508.
(5) Mancini, G.; Sanna, N.; Barone, V.; Migliorati, V.; D'Angelo, P.; Chillemi, G. *J. Phys. Chem. B* **2008**, *112*, 4694–4702.
(6) D'Angelo, P.; Migliorati, V.; Mancini, G.; Chillemi, G. *J. Phys. Chem. A* **2008**, *112*, 11833–11841.
(7) D'Angelo, P.; Zitolo, A.; Migliorati, V.; Mancini, G.; Persson, I.; Chillemi, G. *Inorg. Chem.* **2009**, *48*, 10239–10248.
(8) Ohtaki, H.; Radnai, T. *Chem. Rev.* **1993**, *93*, 1157–1204.
(9) D'Angelo, P.; Di Nola, A.; Filipponi, A.; Pavel, N. V.; Roccatano, D. *J. Chem. Phys.* **1994**, *100*, 985–994.
(10) Tanida, H.; Sakane, H.; Watanabe, I. *J. Chem. Soc., Dalton Trans.* **1994**, *15*, 23212326.
(11) Beudert, R.; Bertagnolli, H.; Zeller, M. *J. Chem. Phys.* **1997**, *106*, 88418848.
(12) Wallen, S. L.; Palmer, B. J.; Pfund, D. M.; Fulton, J. L.; Newville, M.; Ma, Y. J.; Stern, E. A. *J. Phys. Chem. A* **1997**, *101*, 9632–9640.
(13) Ferlat, G.; Miguel, A. S.; Jal, J. F.; Soetens, J. C.; Bopp, P. A.; Daniel, I.; Guillot, S.; Hazemann, J. L.; Argoud, R. *Phys. Rev. B* **2001**, *63*, 134202/1–134202/9.
(14) Filipponi, A.; De Panfilis, S.; Oliva, C.; Ricci, M. A.; D'Angelo, P.; Bowron, D. T. *Phys. Rev. Lett.* **2003**, *91*, 165505/1–165505/4.
(15) Bowron, D. T. *J. Phys.: Conf. Ser.* **2009**, *190*, 012022/1–012022/10.
(16) Bopp, P. In *The Physical Chemistry of Aqueous Solution*; M.-C. Belliment-Funel, Neilson, G. W., Eds.; Reidel: Dordrecht, The Netherlands, 1987.

Published on Web 04/12/2010

regime of water while Filipponi et al.[14] investigated the pressure dependence of the Br−O radial distribution function up to 2.8 GPa. Merkling et al.[17] derived optimized geometries of $[Br(H_2O)_n]^-$ clusters ($1 \leq n \leq 8$) from quantum chemical calculations, and, to reproduce the X-ray absorption near edge structure (XANES) spectra in a satisfactory way, they had to consider statistical fluctuations, which in their case were obtained from snapshots of the Monte Carlo simulations. The latter improvement underlines the crucial role of temperature and the complexity of the problem, which is already implicit from the spread of coordination numbers and distances. Because their analysis was limited to the first shell, Merkling et al.'s[17] simulations are not sufficient to understand the dynamics of hydration, including exchange of water molecules with the bulk. Very recently, time-resolved X-ray absorption spectroscopy has been used to observe the transient species generated by one-photon detachment of an electron from aqueous bromide.[18] A laser pulse of 200 nm has been used to modify the Br^- electronic structure, while X-ray pulses with a duration of 80 ps have been used as probe. The water shell organization has been found to vary upon electronic structure changes but a quantitative analysis of the solvent shell reorganization relies on a clear description of the solvation shell structure around Br^- prior to laser excitation.

Even if many quantum simulations have been carried out on cluster models of water molecules around the halides,[17,20,21] in general, only few simulations (classical, semiclassical, or quantum) have been compared with experimental observables. Recently, Raugei and Klein[19] reported Density Functional Theory (DFT)-based Car−Parrinello MD simulations of a box of 31 water molecules and either one HBr molecule or a Br^- ion. They found a rather structured and asymmetric solvation shell, at variance with the classical MD results.

With regards to structural studies of ion hydration in dilute solutions, EXAFS spectroscopy is the structural probe of choice; because of its intrinsic chemical specificity and short-range sensitivity, this technique measures a less complex correlation function, as compared to X-ray and neutron diffraction, that contains accurate structural information on the first shell hydration structure. However, a proper extraction of the structural parameters from the EXAFS experimental signal relies on the use of reliable starting models that are usually obtained from theoretical calculations. Here we use a combination of state of the art DFT-based MD simulations and EXAFS spectroscopy to develop new understanding of the hydration structure of Br^- aqua ions. In particular, dispersion forces have been accounted for in our DFT-based MD simulations using dispersion-corrected atom-centered pseudopotentials (DCACP)[22] for water.[23] The new improved ion water radial distribution functions have been used as starting model in the analysis of the EXAFS data, and this combined approach allowed us to gain new insights into the structural and dynamical properties of the Br^- hydration complexes.

2. Experimental Section

2.1. Classical Molecular Dynamics Simulation. The classical MD simulation of the bromide ion in aqueous solution has been carried out with the GROMACS package.[24] The OPLS[25] and TIP3P[26] parameters were used for the ion and the water model, respectively. The system was composed of one bromide ion and 819 water molecules in a cubic box, using periodic boundary conditions. The system has been simulated in an NVT ensemble, where the temperature was kept fixed at 300 K using the Berendsen method[27] with a coupling constant of 0.1 ps. A cutoff of 9 Å has been used for the nonbonded interactions, using the particle mesh Ewald method to calculate the long-range electrostatic interactions.[28] The simulation has been carried out for 13 ns, with a time step of 1 fs. The first 3 ns have been used for equilibration and discarded in the following analyses.

2.2. Car−Parrinello Molecular Dynamics Simulation. The Kohn−Sham formulation of DFT, which is implemented in the CPMD code, has been used in the Car−Parrinello Molecular Dynamics (CPMD) simulation.[29] The gradient-corrected BLYP (Becke−Lee−Yang−Parr) functional has been employed.[30] The simulated system consists of one bromide ion and 90 water molecules in a periodic cubic box with 14 Å edge. The Martins−Troullier pseudopotential was used for the bromide ion, while the core electrons of oxygen and hydrogen atoms have been treated using the recently developed DCACP.[22] Recent calculations using DCACP pseudopotentials in combination with the BLYP functional have shown improved structural and dynamical properties of liquid water.[23] The electronic wave functions have been expanded in a plane wave basis set up to an energy cutoff of 70 Ry. The simulation was performed using the Car−Parrinello approach,[31] with a fictitious mass associated with the electronic degrees of freedom of 400 au. After an equilibration time of 2 ps, during which thermalization at 300 K has been achieved by a Nosé−Hoover thermostat with a coupling frequency of 1500 cm^{-1}, the equations of motion have been integrated with a time step of 4 au, for a total simulation time of 4.4 ps in the NVE ensemble. No drift in the electronic kinetic energy was observed during the total simulation time. Note that a homogeneous background charge has been used to compensate for the negative charge of the bromide ion.[32]

2.3. Structural and Dynamic Analysis from MD Simulations. The structural properties of the bromide ion aqueous solutions

(17) Merkling, P. J.; Ayala, R.; Martinez, J. M.; Pappalardo, R. R.; Marcos, E. S. *J. Chem. Phys.* **2003**, *119*, 6647–6654.
(18) Elles, C. G.; Shkrob, I. A.; Crowell, R. A.; Arms, D. A.; Landahl, E. C. *J. Chem. Phys.* **2008**, *128*, 061102/1–061102/4.
(19) Raugei, S.; Klein, M. L. *J. Chem. Phys.* **2002**, *116*, 196–202.
(20) Cappa, C. D.; Smith, J. D.; Wilson, K. R.; Messer, B. M.; Gilles, M. K.; Cohen, R. C.; Saykally, R. J. *J. Phys. Chem. B* **2005**, *109*, 7046–7052.
(21) Heuft, J. M.; Meijer, E. J. *J. Chem. Phys.* **2005**, *123*, 094506/1–094506/5.
(22) von Lilienfeld, O. A.; Tavernelli, I.; Rothlisberger, U.; Sebastiani, D. *Phys. Rev. Lett.* **2004**, *93*, 153004/1–153004/4.
(23) Lin, I. C.; Seitsonen, A. P.; Coutinho-Neto, M. D.; Tavernelli, I.; Rothlisberger, U. *J Phys. Chem. B.* **2009**, *113*, 1127–1131.
(24) van der Spoel, D.; Lindahl, E.; Hess, B.; van Buuren, A. R.; Apol, E.; Meulenhoff, P. J.; Tieleman, D. P.; Sijbers, T. M.; Feenstra, K. A.; van Drunen, R.; Berendsen, H. J. C. *Gromacs User Manual*, version 3.3; Department of Biophysical Chemistry, University of Groningen: Groningen, The Netherlands, 2005; www.gromacs.org.
(25) Lybrand, T. P.; Ghosh, I.; McCammon, J. A. *J. Am. Chem. Soc.* **1985**, *107*, 7793–7794.
(26) Jorgensen, W. L.; Chandrasekhar, J.; Madura, J. D.; Impey, R. W.; Klein, M. L. *J. Chem. Phys.* **1983**, *79*, 926–935.
(27) Berendsen, H. J. C.; Postma, J. P. M.; Di Nola, A.; Haak, J. R. *J. Chem. Phys.* **1984**, *81*, 3684–3690.
(28) (a) Darden, T.; York, D.; Pedersen, L. *J. Chem. Phys.* **1993**, *98*, 10089–10092. (b) Essmann, U.; Perera, L.; Berkowitz, M. L.; Darden, T.; Lee, H.; Pedersen, L. G. *J. Chem. Phys.* **1995**, *103*, 8577–8592.
(29) Hutter, J.; Alavi, A.; Deutch, T.; Bernasconi, M.; Goedecker, S.; Marx, D.; Tuckerman, M.; Parrinello, M. *CPMD*: MPI für Festkörperforschung and IBM Zurich Research Laboratory: Stuttgart, Germany, 1995−1999.
(30) (a) Becke, A. D. *Phys. Rev. A* **1988**, *38*, 3098–3100. (b) Lee, C.; Yang, W.; Parr, R. G. *Phys. Rev. B* **1988**, *37*, 785–789.
(31) Car, R.; Parrinello, M. *Phys. Rev. Lett.* **1985**, *55*, 2471–2474.
(32) Hummer, G.; Pratt, L. R.; Garcia, A. E. *J. Phys. Chem. A* **1998**, *102*, 7885–7895.

are described in terms of radial distribution functions, $g_{Br-O}(r)$ and $g_{Br-H}(r)$:

$$g_{AB}(r) = \frac{\langle \rho_B(r) \rangle}{\langle \rho_B \rangle_{local}} = \frac{1}{N_A \langle \rho_B \rangle_{local}} \sum_{i \in A}^{N_A} \sum_{i \in B}^{N_B} \frac{\delta(r_{ij} - r)}{4\pi r^2} \quad (1)$$

where $\langle \rho_B(r) \rangle$ is the particle density of type B at distance r around type A, and $\langle \rho_B \rangle_{local}$ is the particle density of type B averaged over all spheres around particle A with radius r_{max} (half the box length).

Angular distribution functions have been calculated for three different angles: the angle formed by two Br−O vectors in the first shell (labeled as ψ), the angle formed by the water molecule dipole and the Br−O vector direction (labeled as ϕ), and the angle formed by the Br−O and Br−H vectors (labeled as ω).

The mean residence time of water molecules in the first hydration shell has been evaluated, for the classical MD simulation, using the approach proposed by Impey et al.[33] This method is based on the definition of a survival probability function $P_j(t, t_n, t^*)$, which takes the value one if the water molecule j lies within the first hydration shell at both time steps t_n and $t + t_n$ and does not leave the coordination shell for any continuous period longer than t^*, otherwise it is zero. From P_j it is possible to evaluate the time-dependent coordination number (or survival function) $n_{hyd}(t)$:

$$n_{hyd}(t) = \frac{1}{N_t} \sum_{n=1}^{N_t} \sum_j P_j(t_n, t, t*) \quad (2)$$

where N_t is the total number of steps, and the summation goes over all water molecules. At long times, $n_{hyd}(t)$ decays in an exponential fashion, with a characteristic correlation time, which defines the residence time of the water molecules in the first hydration shell. A second approach, called the "direct method" and proposed by Hofer et al.,[34] has been also applied. This method scans the whole trajectory for movements of the ligands, either entering or leaving the first coordination shell. Whenever a ligand crosses the boundaries of the shell, its further path is followed, and if its new placement outside or inside the shell lasts for more than a chosen t^*, the event is accounted for as a "real" exchange process. Thus t^* has the same role as in the Impey procedure. The water residence time τ_d is then calculated as:

$$\tau_d = \frac{t_{sim} \overline{n}}{N_{ex}} \quad (3)$$

where t_{sim} is the total simulation time, $\overline{n}$ is the average first shell coordination number, and N_{ex} is the number of "real" solvent exchanges between the first hydration shell and the rest of the solvent. All the structural and dynamic analyses of the MD simulations have been carried out using in-house written codes.

2.4. X-ray Absorption Measurements. K-edge X-ray absorption spectra were recorded at the BM29 beamline of the European Synchrotron Radiation Facility (ESRF-Grenoble).[35] The sample was a 0.1 M RbBr aqueous solution kept in a cell with Kapton windows. The absorption coefficient was measured in transmission mode, and the monochromator was equipped with two flat Si(311) crystals for high-energy operation with excellent resolution. To reduce harmonic contamination, the crystals were kept slightly detuned with a feedback system. The incident and transmitted fluxes were monitored by ionization chambers filled with Kr gas. The storage ring was operating in 2/3 fill mode with a typical current of 200 mA after refill.

2.5. EXAFS Data Analysis. In conventional EXAFS data analysis of disordered systems the $\chi(k)$ signal is represented by the equation:

$$\chi(k) = \int_0^\infty dr\, 4\pi\rho r^2\, g(r)\, A(k,r)\, \sin[2kr + \phi(k,r)] \quad (4)$$

where $A(k,r)$ and $\phi(k,r)$ are the amplitude and phase functions, respectively, and ρ is the density of the scattering atoms. $\chi(k)$ theoretical signals can be calculated by introducing in eq 4 the model radial distribution functions obtained from MD simulations. It is well-known that the atomic background of several elements contains important contributions associated with the opening of multielectron excitation channels. Here the background function used to extract the $\chi(k)$ experimental signals has been modeled by means of step-shaped functions accounting for the 1s4p, 1s3d, and 1s4p double-electron resonances, as determined for HBr and TMABr.[36−38]

Both the Br−O and Br−H $g(r)$'s obtained from the two simulations have been used to calculate the single scattering first shell $\chi(k)$ theoretical signal, as the ion-hydrogen interactions have been found to provide a detectable contribution to the EXAFS spectra of several metal ions in aqueous solutions.[9,39−41] Comparison of the theoretical and experimental total $\chi(k)$ signals allows the reliability of the $g(r)$'s, and consequently of the theoretical scheme and the water model used in the simulations, to be checked.

The EXAFS theoretical signals have been calculated by means of the GNXAS program and a thorough description of the theoretical framework can be found in ref 42. Phase shifts, $A(k,r)$ and $\phi(k,r)$, have been calculated starting from one of the MD configurations, by using muffin-tin potentials and advanced models for the exchange-correlation self-energy (Hedin−Lundqvist).[43] The values of the muffin-tin radii are 0.2 Å, 0.9 Å, and 2.3 Å for hydrogen, oxygen, and bromine, respectively. These radii correspond to an overlap between the bromine and hydrogen atoms of about 10%. Anyhow, we have checked that there are no detectable variations of the theoretical signals in the EXAFS region when the muffin-tin radii are reduced until tangency is reached. Inelastic losses of the photoelectron in the final state have been accounted for intrinsically by a complex potential. The imaginary part also includes a constant factor accounting for the core-hole width.

3. Results

3.1. Hydration Structure from MD Simulations. Structural arrangements of water molecules around the bromide ion are characterized by the Br−O and Br−H radial distribution functions, and the results obtained from the classical MD and CPMD simulations are depicted in Figure 1. In both cases, the presence of a nonzero first minimum in the Br−O $g(r)$'s and of a second minimum in the Br−H $g(r)$'s indicates that the first solvation shell is not well-defined, and several exchange events take place

(33) Impey, R. W.; Madden, P. A.; McDonald, I. R. *J. Phys. Chem.* **1983**, *87*, 5071–5083.
(34) Hofer, T. S.; Tran, H. T.; Schwenk, C. F.; Rode, B. M. *J. Comput. Chem.* **2004**, *25*, 211–217.
(35) Filipponi, A.; Borowski, M.; Bowron, D. T.; Ansell, S.; De Panfilis, S.; Di Cicco, A.; Itiè, J.-P. *Rev. Sci. Instrum.* **2000**, *71*, 2422–2432.
(36) D'Angelo, P.; Di Cicco, A.; Filipponi, A.; Pavel, N. V. *Phys. Rev. A* **2000**, *71*, 2055–2063.
(37) D'Angelo, P.; Pavel, N. V. *Phys. Rev. B* **2001**, *64*, 233112/1–233112/4.
(38) Burattini, E.; D'Angelo, P.; Giglio, E.; Pavel, N. V. *J. Phys. Chem.* **1991**, *95*, 7880–7886.
(39) D'Angelo, P.; Pavel, N. V.; Roccatano, D.; Nolting, H.-F. *Phys. Rev. B* **1996**, *54*, 12129–12138.
(40) D'Angelo, P.; De Panfilis, S.; Filipponi, A.; Persson, I. *Chem.—Eur. J.* **2008**, *14*, 3045–3055.
(41) D'Angelo, P.; Benfatto, M.; Della Longa, S.; Pavel, N. V. *Phys. Rev. B* **2002**, *66*, 064209–064215.
(42) Filipponi, A.; Di Cicco, A.; Natoli, C. R. *Phys. Rev. B* **1995**, *52*, 15122–15134.
(43) Hedin, L.; Lundqvist, B. I. *J. Phys. C* **1971**, *4*, 2064–2083.

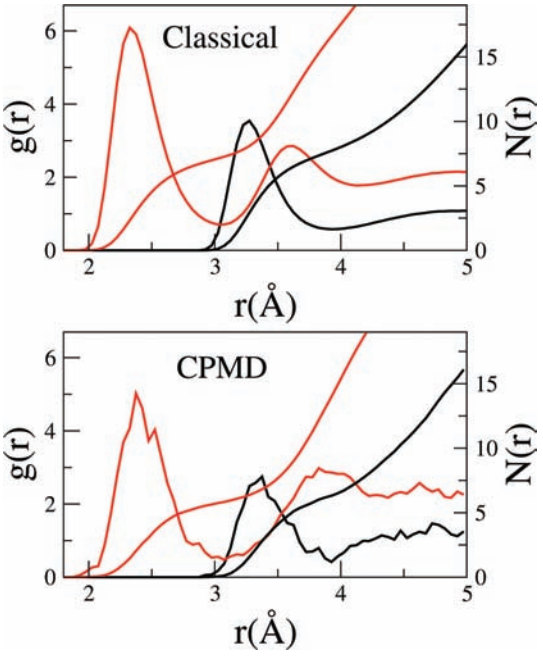

Figure 1. Br−O (black line) and Br−H (red line) radial distribution functions obtained from the classical MD and CPMD simulations. Running integration numbers are also shown.

between the first and second hydration sphere. Moreover, the Br−H $g(r)$'s show the presence of two peaks, the former at shorter distances and the latter at longer distances as compared to the Br−O $g(r)$ first maxima, meaning that the first shell water molecules orient only one hydrogen atom toward the bromide ion. This result is not obvious for the classical MD simulation since in the classical framework the anion is represented by a negative charge having electrostatic and Lennard-Jones interactions with the water molecules. This simple description, which completely neglects the ion polarizability, could have led to an overestimation of the ion−water dipole interactions, giving rise to a symmetric arrangement with the two hydrogen atoms pointing toward the anion almost at the same distance.

The main difference between the classical and the CPMD simulation is the Br-water first shell distance. Inspection of Figure 1 reveals that the rising edges and the first peak positions are shifted toward shorter distances in the classical case both for the Br−O and Br−H $g(r)$'s. This result is a first indication that the pair potentials used in the classical approach are more rigid giving rise to a first hydration shell which is more tightly bound to the bromide ion. Note that also the intensity of the classical $g(r)$ peaks is higher as compared to the CPMD one. This overall tendency is reflected in the number of water molecules present in the first hydration shell of the anion as obtained from the running integration numbers of the Br−O $g(r)$'s that are 7.6 and 6.5 up to the first minima (3.9 Å in both cases) for the classical and CPMD simulations, respectively (see Figure 1). These results are at variance with those of Raugei and Klein[19] who found a first shell coordination number of 5.1. The present CPMD simulation differs from that carried out by Raugei and Klein in the number of water molecules (we use 90 solvent molecules while Raugei and Klein use 31), and in the choice of the exchange-correlation functional (BLYP here vs HCTH) as well as of the pseudopotentials for water (DCACP here vs Martins−Troullier for the oxygen atoms and a von Barth−Car analytical pseudopotential for hydrogen).

Table 1. Comparison of the Structural Parameters for the Bromide Solvation Shell Obtained in Different Experimental and Theoretical Studies[a]

R_{Br-O}(Å)	N	technique	ref.
3.34	6.9	EXAFS	9
3.19	6	EXAFS	10
3.35	7.4	AXS	11
3.40(0.03)	6.9(1.5)	EXAFS	12
3.4	6.9	EXAFS	13
3.4		EXAFS	14
3.3	6.3	ND+EXAFS	15
3.37	5.1	CPMD	19
3.33(0.02)	6.5(0.3)	CPMD	this work
3.270(0.003)	7.6(0.5)	classical MD	this work

[a] R_{Br-O} is the bromide-oxygen first shell distance while N is the average first shell coordination number. The abbreviation AXS refers to Anomalous X-ray Scattering, and ND to Neutron Diffraction.

To see how the results obtained in this study compare with other investigations of the bromide hydration, we report in Table 1 the bromide-oxygen first shell distance and the average first shell coordination number obtained in different experimental and theoretical studies. As far as the first shell distance is concerned, the results of our CPMD simulation compare well with previous EXAFS studies, as well as with the theoretical results obtained by Raugei and Klein.[19] It is interesting to note that apart from the oldest study by Tanida et al.,[10] all of the EXAFS determinations compare quite well within the usual statistical error of this technique. On the other hand the first shell distance of our classical trajectory is too short as compared with previous determinations. Some variation is found in the hydration numbers between the various studies. However, the average coordination number calculated from our CPMD simulation is in good agreement with previous EXAFS determinations, at variance with the coordination numbers obtained both by Raugei and Klein[19] and with our classical MD simulation.

A deeper insight can be gained by defining an instantaneous coordination number n, as the number of oxygen atoms at a distance shorter than the Br−O $g(r)$ first minimum, and analyzing its variation along the simulations. The coordination number distributions are shown in Figure 2. In both trajectories the bromide ion transits among several coordination numbers, but the distributions obtained from the two simulations are very different. The dominant species existing in solution are indeed seven- and eight-fold hydration complexes in the classical MD simulation, while only six-fold complexes in the CPMD simulation.

The geometrical arrangement of the first shell water molecules around the bromide ion can be evaluated by looking at the angular distribution functions of the O−Br−O ψ angle, plotted in Figure 3 as $1 - \cos \psi$. The ψ distributions obtained from the classical and CPMD trajectories drop to zero for $1 - \cos \psi$ values lower than 0.25, showing that ψ angle values smaller than 41° are prohibited in both simulations. As far as the CPMD trajectory is concerned, no clear peaks can be observed in the ψ distribution, showing the absence of a well-defined configuration of water molecules around the

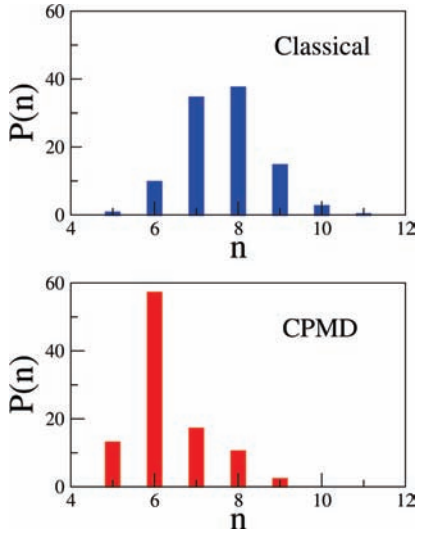

Figure 2. Instantaneous coordination number (n) distribution obtained from the classical MD and CPMD simulations.

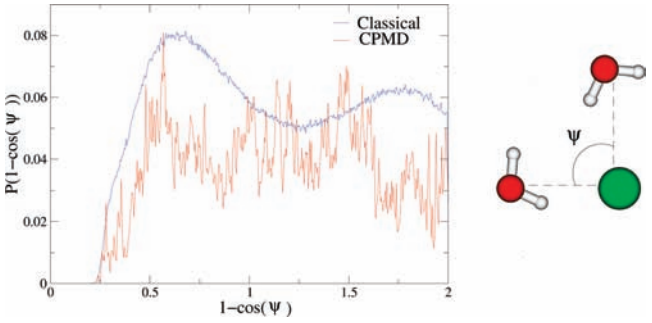

Figure 3. O−Br−O ψ angular distribution functions obtained from the classical MD and CPMD simulations.

bromide ion. This finding differs from the results obtained by Raugei and Klein[19] where the water molecules occupy well-defined positions around the Br^- ion (the most stable first shell configuration has a 4 + 2 structure where four water molecules coordinate the anion according to a hypothetical square pyramidal geometry, and the other two molecules coordinate it on the other side). Conversely, in the classical MD simulation two broad peaks are found at $1 - \cos\psi = 0.63$ and $1 - \cos\psi = 1.78$ ($\psi = 68.3°$ and $\psi = 141.3°$, respectively), indicating the existence of a more structured coordination sphere.

The orientation of a single water molecule in the first hydration shell can be inferred from the distribution function of ϕ angles (Figure 4). In both simulations the ϕ distributions show a well-defined peak, and the maxima are located at $\phi = 49.5°$ for the classical simulations, and $\phi = 55.3°$ for the CPMD simulation. These distributions are consistent with a nearly linear Br- - -H−O hydrogen bond, in agreement with the results of Raugei and Klein[19] and with previous calculations on anions in water.[8] The broader and lower-intensity ϕ distribution obtained from the CPMD simulation provides a further proof of the higher flexibility of the first hydration shell in agreement with the above-mentioned results. The distributions of the ω angle are shown in Figure 5. The sharp peak located at 0° indicates that one hydrogen atom of the first shell is strongly bound to the anion in a linear Br- - -H−O

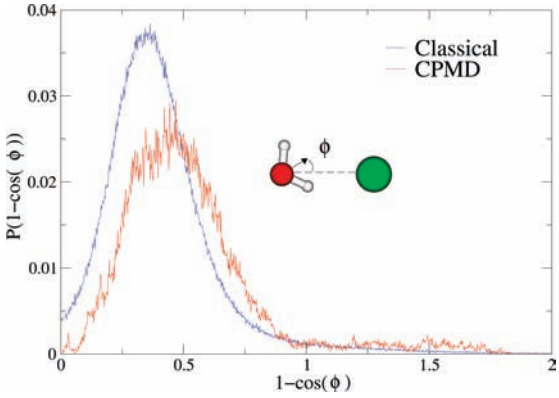

Figure 4. Angular distribution functions of the ϕ angle between the water dipole and the Br−O vector direction obtained from the classical MD and CPMD simulations.

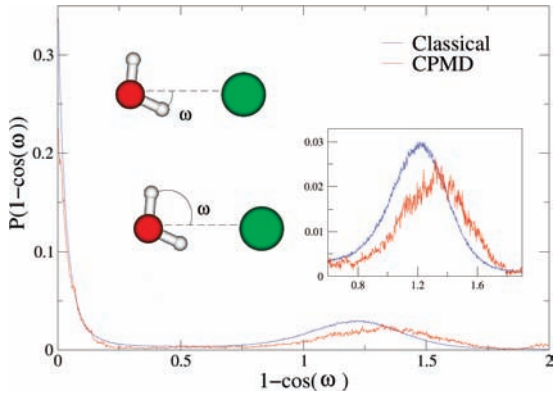

Figure 5. ω Angular distribution functions obtained from the classical MD and CPMD simulations.

configuration. The second hydrogen atom, which is less tightly bound and more free to rotate, is responsible for the second peak which is less intense and broader than the first one. As evident from the inset of Figure 5 , the maxima of the second peak are found at ω values of 103.2° for the classical and of 109.3° for the CPMD trajectory, coherently with the linear Br- - -H−O configuration.

Even if the water molecules do not occupy well-defined positions around the ion, as evidenced from the ψ angular distribution function analysis, it is possible to evaluate the asymmetry of the first coordination shell by analyzing the distance between the center of mass of the first hydration shell cage and the bromide ion (R_{cage}) (see Figure 6). From Figure 6 a slight asymmetry of the first hydration shell can be inferred, with the asymmetry being more pronounced in the CPMD trajectory (the R_{cage} distribution peaks are located at 0.40 and 0.58 Å for the classical and CPMD simulations, respectively). The stronger asymmetry found by Raugei and Klein[19] is due to the highly asymmetric 4 + 2 first shell structure which resulted from their CPMD simulation. The asymmetry of the first coordination is responsible for the presence of an induced net dipole moment on the bromide ion. The anion dipole moment has been calculated from the CPMD trajectory with respect to the anion nucleus position, using the maximally localized Wannier function centers.[44,45] The positions of the Wannier centers are

(44) Marzari, N.; Vanderbilt, D. *Phys. Rev. B* **1997**, *56*, 12847–12865.

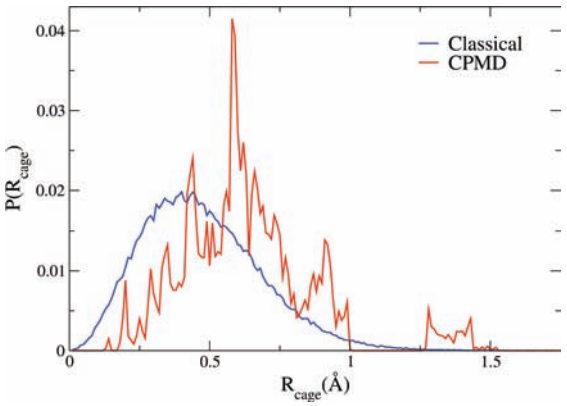

Figure 6. Distributions of the distance between the center of mass of the first hydration shell cage and the bromide ion (R_{cage}) obtained from the classical MD and CPMD simulations.

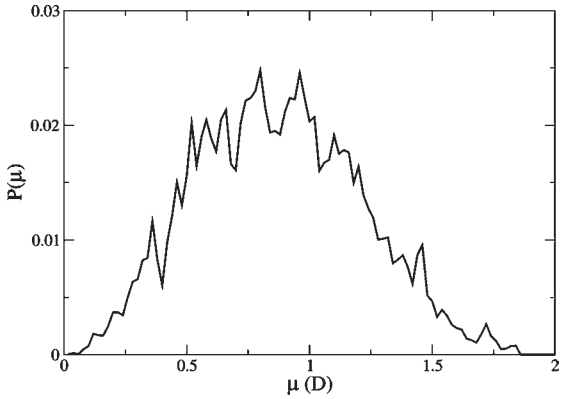

Figure 7. Distribution of the bromide dipole moment μ calculated from the CPMD simulation.

representative of the location of the electrons in the system, and, as a consequence, it is possible to compute the molecular (or atomic) dipole moment assuming that the electrons belong to the nearest neighbor atom. The peak of the anion dipole moment distribution is found at $\mu = 0.85$ D (see Figure 7), indicating that the bromide electron density is strongly influenced by the presence of the surrounding water molecules and that the inclusion of polarization effects is essential to provide a correct description of the anion-water interactions.

The flexible and unstructured layout of the bromide ion first solvation shell is reflected in its dynamical behavior. Several water exchange events between the first and the second hydration shell have been observed during the two simulations, and the rate of the water exchange processes has been evaluated by means of mean residence time of the water molecules in the first hydration shell. This property has been determined using both the Impey et al.[33] and the direct method[34] for the classical simulation and, because of the short simulation time, only with the direct method for the CPMD one. The problems encountered when trying to apply the Impey procedure for calculating the residence time from relatively short MD simulations have been already pointed out in the literature,[34] and are related to the difficulty of fitting the Impey survival function $n_{hyd}(t)$ to the required exponential form. On the other hand, it is always possible to count the number of exchange processes between water molecules belonging to the first and second coordination shell during a simulation, and then to determine the residence time by means of the direct method. However, it is important to bear in mind that also with the latter method the shorter the simulation time, and consequently the number of exchange processes, the higher the error on the calculated residence time values. The results of this analysis are listed in Table 2 for t^* values of 0.0, 0.5, and 2.0 ps. A proper choice of the t^* parameter is fundamental for systems with a very flexible first hydration shell, where the definition of the first hydration shell can be somehow arbitrary, as in the present case. We find that the calculated residence times are strongly dependent on the choice of t^* with both procedures, the dependence being stronger for the direct method. A t^* value of 0.5 ps has been found to be the more appropriate choice,[34] as it corresponds to the average lifetime of a water−water hydrogen bond. With this choice, the residence time calculated from the CPMD simulation is longer as compared to the classical one. However, the results obtained from both simulations are in the order of magnitude of the experimental determination.[16] Note that the residence time calculated from our CPMD simulation with a t^* value of 2.0 ps approaches the value obtained by Raugei and Klein using the Impey method and the same t^*, for the HBr aqueous solution (19 ps).[19] The same authors suggested for the Br^- aqueous solution a slightly lower value of the residence time, as compared to the HBr one.

Table 2. Residence Times (ps) of Water Molecules in the First Coordination Shell of the Bromide Ion, Calculated Using the Impey Procedure (τ_I)[33] and the Direct Method (τ_d)[34] As a Function of the t^* Parameter, for the Classical MD and CPMD Simulations[a]

	$t^* = 0.0$ ps			$t^* = 0.5$ ps			$t^* = 2.0$ ps		
trajectory	τ_I	τ_d	N_{ex}	τ_I	τ_d	N_{ex}	τ_I	τ_d	N_{ex}
classical	2.4	0.7	113862	3.8	2.6	28939	5.8	4.7	16305
CPMD		0.4	77		5.7	5		14.3	2

[a] N_{ex} is the number of exchange events observed during the total simulation time.

3.2. Comparison with the EXAFS Experimental Data. Direct comparison of the MD structural results with the EXAFS experimental data allows the accuracy of the simulations to be assessed. $\chi(k)$ theoretical signals have been calculated by means of eq 4 starting from the classical and CPMD Br−H and Br−O $g(r)$'s. The structural parameters derived from the simulations were kept fixed during the EXAFS analysis. In this way the first hydration shell structure obtained from the simulations can be directly compared with the experimental data, and the validity of the theoretical frameworks can be assessed. In the upper panels of Figure 8, the comparison between the experimental signal and the theoretical curves is reported for the classical MD and CPMD simulations (left and right panels, respectively). The first two curves from the top are the Br−H and Br−O first shell contributions calculated by inserting in eq 4 the MD $g(r)$'s without any adjustable parameter, while the remainder of the figures shows the total theoretical signal compared with the experimental spectrum, and the resulting residuals.

(45) Silvestrelli, P. L.; Marzari, N.; Vanderbilt, D.; Parrinello, M. *Solid State Commun.* **1998**, *107*, 7–11.

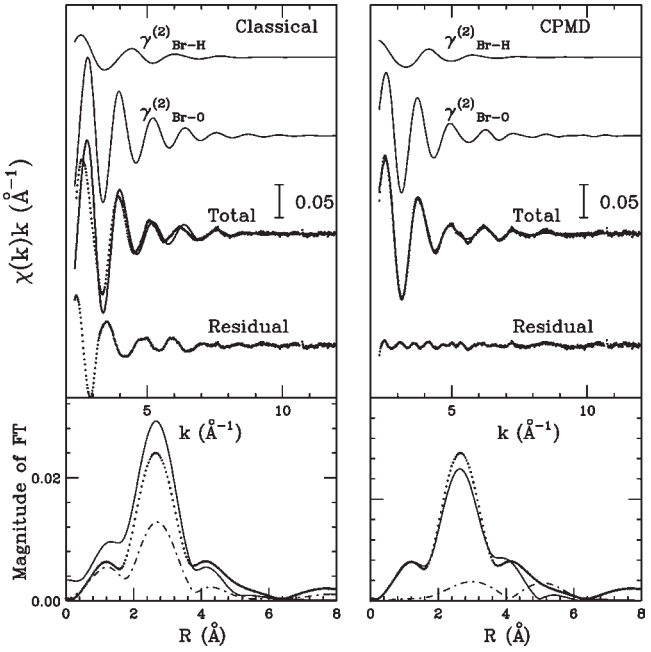

Figure 8. Upper panels: Comparison between the EXAFS theoretical signals (solid line) calculated from the classical MD and CPMD Br−O and Br−H $g(r)$'s and experimental data (dotted line). The residual signals are also shown. Lower panels: Nonphase-shifted corrected Fourier transforms of the experimental data (dotted line), of the theoretical signals (solid line), and of the residual curves (dot-dashed line).

In the case of the classical MD simulation the agreement between the calculated and experimental EXAFS spectra is quite poor, and the presence of a leading frequency can be clearly identified in the residual curve. This behavior is due to the short value of the average Br−H and Br−O first shell distances as compared to the experimental results. This finding is reinforced by the Fourier transform (FT) moduli of the EXAFS $\chi(k)$ theoretical, experimental, and residual signals shown in the lower panels of Figure 8. The FTs have been calculated in the k-range 3.0−7.5 Å^{-1} with no phase shift correction applied. The theoretical first-neighbor peak obtained from the classical simulation is found to be broader and shifted toward shorter distances than predicted by the experiment. Conversely, the theoretical $\chi(k)$ signal calculated from the CPMD $g(r)$'s matches the experimental data very well, and a good agreement is found also looking at the FTs. Therefore, the structural and dynamical information derived from the CPMD simulation is basically correct.

Finally, it is interesting to note that even if the Br−O two body signal provides the most important contribution to the total $\chi(k)$ function, the hydrogen atoms in the first hydration shell give rise to a sizable contribution especially in the k region below 6 Å^{-1}. The importance of the hydrogen contribution to the EXAFS spectra of metal cations in aqueous solution has been pointed out in several previous works.[5,6,46] However, to the best of our knowledge, this is the first time that the hydrogen scattering is included in the EXAFS analysis of anion aqueous solutions. Note that a reliable calculation of the contribution associated with the hydrogen atoms in the first hydration shell relies on a proper description of the anion−water and water−water interaction in the MD simulations. In this context use of advanced methods in the CPMD setup has been found to be essential to provide a correct description of the structural properties of the Br^- hydration shells.

3.3. Discussion. In the present work we have investigated the hydration properties of the Br^- ion by means of classical MD and Car−Parrinello simulations with DCACP pseudopotentials for water. The reliability of the theoretical framework has been assessed with EXAFS experimental data. We have found that the CPMD $g(r)$'s deliver a better agreement with the experimental data than the classical simulations. In general, halide ion−water interactions, excluding fluoride, are weaker than those of most cations and energetically comparable with the water−water interactions in bulk water. Therefore, the structural properties of the solvent significantly increase their role, and, as a result, a correct description of the halide hydration properties can be obtained only with theoretical methods able to reproduce the delicate compromise between solute−solvent and solvent−solvent interactions. Moreover, it has been shown that the polarizability of the anion may be one of the most important factors in determining the structure of gas phase clusters.[47,48] As far as the aqueous solutions are concerned, polarizable models have been used in classical MD simulations providing results in qualitative agreement with the experimental data. Nevertheless, since there are no direct measurements of halogen ion polarizability in aqueous solution it is not easy to include in a reliable fashion polarization effects in classical simulations.[49] Conversely, DFT-based molecular dynamics is able to describe the dynamics of the system in a self-consistent fashion, taking into account in a natural way polarization and many-body interactions. It is important to stress that a possible shortcoming of the DFT-based simulations stems from the quality of the water−water intermolecular interactions. Previous studies have shown that the outcome of DFT-based MD simulations of liquid water is very sensitive to the particular choice of the functional[50] and basis set.[51] Water computed at the DFT level within the generalized gradient approximation (GGA) for the exchange-correlation functional is generally overstructured and diffuses 1 order of magnitude more slowly than experimentally determined. Hybrid functionals improve the predictions slightly,[52] and the reason for such discrepancies was the subject of recent theoretical studies.[23,53−55] It has been shown that improving

(46) D'Angelo, P.; Barone, V.; Chillemi, G.; Sanna, N.; Meyer-Klauke, W.; Pavel, N. V. *J. Am. Chem. Soc.* **2002**, *124*, 1958–1967.
(47) Stuart, S. J.; Berne, B. J. *J. Phys. Chem.* **1996**, *100*, 11934–11943.
(48) Dang, L. X.; Garrett, B. C. *J. Chem. Phys.* **1993**, *99*, 2972–2977.
(49) Tongraar, A.; Rode, B. M. *Phys. Chem. Chem. Phys.* **2003**, *5*, 357–362.
(50) VandeVondele, J.; Mohamed, F.; Krack, M.; Hutter, J.; Sprik, M.; Parrinello, M. *J. Chem. Phys.* **2005**, *122*, 014515/1–014515/6.
(51) Lee, H. S.; Tuckerman, M. E. *J. Chem. Phys.* **2006**, *110*, 154507/1–154507/14.
(52) Todorova, T.; Seitsonen, A. P.; Hutter, J.; Kuo, I. F. W.; Mundy, C. J. *J. Phys. Chem. B* **2006**, *110*, 3685–3691.
(53) Leung, K.; Rempe, S. B. *Phys. Chem. Chem. Phys.* **2006**, *85*, 2153–2162.
(54) Santra, B.; Michaelides, A.; Scheffler, M. *J. Chem. Phys.* **2009**, *131*, 124509/1–124509/9.
(55) Schmidt, J.; VandeVondele, J.; Kuo, I.-F. W.; Sebastiani, D.; Siepmann, J. I.; Hutter, J.; Mundy, C. J. *J. Phys. Chem. B* **2009**, *113*, 11959–11964.

the description of the van der Waals interactions in DFT-GGA leads to a softening of the liquid water's structure with a consequent improvement of the agreement with experiments,[23,55] and therefore in the present work we have resorted to the use of DCACP pseudopotentials in combination with the BLYP functional. This new improved approach has furnished different dynamical and structural results as compared to a previous DFT-simulation on Br^- in aqueous solution carried out by Raugei and Klein.[19] In particular, we have found that the anion first solvation shell is formed on average by 6.5 water molecules with a Br−O first shell distance of 3.33 Å. The Br^- hydration sphere is much less structured and asymmetric as compared to the previous simulation,[19] in better agreement with the experimental data. Moreover, the Br^- anion has been found to be strongly influenced by the presence of surrounding water molecules, and, as a consequence of the asymmetry of the inner solvation shell, it has a net dipole moment close to 0.8 D.

A last remark we would like to make concerns a possible alternative explanation of the overstructured radial distribution function observed in BLYP simulations of pure water which has been recently pointed out in the literature.[53,54] Santra et al.[54] showed that the energy cost to distort water monomers to the geometry adopted in the liquid is underestimated by the BLYP functional. As a consequence the OH bond is too long, leading to stronger hydrogen bonds and to an overstructured liquid phase. These results open new perspectives that deserve further investigations.

In conclusion, we have shown that advanced DFT-based simulation techniques are necessary to provide a proper description of the hydration properties of halide anions. We have also demonstrated that when reliable structural results are used as starting models in the analysis of the EXAFS data, the contribution of the hydrogen atoms to the X-ray absorption spectra of aqueous halide systems can be properly singled out.

Acknowledgment. This work was supported by CASPUR with the Standard HPC Grant 2009 entitled: "A combined X-ray absorption spectroscopy, Molecular Dynamics simulations and Quantum Mechanics calculation procedure for the structural characterization of ill-defined systems". We acknowledge the European Synchrotron Radiation Facility for provision of synchrotron radiation facilities.